

Influence of EPO and graphene nanofillers on mechanical behavior of flax fiber reinforced PLA biocomposite

Jiyas N^{1,2} and K Bindu Kumar^{*1,2}

¹Department of Mechanical Engineering, Government Engineering College,
Barton Hill, Thiruvananthapuram, Kerala 695035, India

²APJ Abdul Kalam Technological University, Thiruvananthapuram, Kerala, India

(Received January 20, 2023, Revised December 17, 2025, Accepted December 18, 2025)

Abstract. Biodegradable materials are the need for the hour and have no exemption for the automotive industry. The proposed work aims to develop a biodegradable green composite using Poly Lactic Acid (PLA) as the polymeric matrix, flax fiber fabric as reinforcement, Epoxidized Palm Oil (EPO) as a plasticizer, and graphene powder as nano fillers. Using the hot compression technique, the solvent-cast composites with 5% EPO and 0.5% graphene nano fillers are fabricated and tested for mechanical strength to suit automobile applications. Tensile, flexural, impact tests and inter laminar shear strength analysis were performed and compared with the composite laminates made of PLA, PLA-EPO, and PLA-EPO-Graphene. Scanning Electron Microscopy (SEM) was used to observe the surface morphology at the rupture part of the tensile samples.

Keywords: bio-degradable composite; epoxidized palm oil; flax fiber; graphene nano powder; natural fibers; poly lactic acid

1. Introduction

The growth of composite manufacturing technology has shown considerable advancements in the application of polymer matrix composites in various engineering applications. Even though these composites are superior to others due to their flexibility, cost, and ease of fabrication but their non-biodegradability is a major drawback. During recent decades, the scientific community has been looking towards sustainable materials to reduce their impact on the environment, hence developing green composites. Biopolymers are compatible with many processing techniques such as injection molding, extrusion, compression molding, etc. Biocomposites are made with superior performance having high renewable contents and are successfully derived from natural fibers and biobased thermosets (Shelly *et al.* 2025, Liu *et al.* 2019). Green composites are fabricated by reinforcing biopolymers with natural fibers like coir, flax, sisal, bamboo fiber, etc. At the same time, starch and Polypropylene (PP), Polystyrene (PS), and Polyethylene (PE) Poly Lactic Acid (PLA) are examples of biopolymers used for the Preparation of Green Composites (PMcClements 2024, Sreekumar and S. Thomas 2008). The Partially and fully biodegradable combinations of natural fibre like jute, sisal-reinforced composites have been prepared with the matrices of synthetic polymers like petroleum (polypropylene (PP)) or natural, polylactic acid (PLA) resources. Experimental results showed that

*Corresponding author, Professor, E-mail: profkbbk@gecbh.ac.in

the tensile and flexural moduli of the PLA composites were higher than respective PP composites (Islam *et al.* 2024, Kandola *et al.* 2018).

The mechanical properties of PLA are in comparison with PP, PS, High Density Polyethylene (HDPE), Polyamide (PA6) are reported (Farah *et al.* 2016). The melting point of PLA is less as reported (V. Sangeetha *et al.* 2016) Many works have been reported using PLA as it is inexpensive, dimensionally stable, and harder (Wang *et al.* 2024, Nurul Fazita *et al.* 2016).

Several studies on hybrid combinations of natural fibers are reported (Islam *et al.* 2024, Srinivasan *et al.* 2014). Izod impact strength test results on abaca reinforced polypropylene composites showed better fiber–matrix interface enhancement in materials with higher resistance to crack formation (Girones *et al.* 2011). Even though green composites are preferred over polymer composites, the lack of proper fiber-matrix adhesion causes the degradation of mechanical properties. Another issue spotted with green composites is the hydrophilic nature of the natural fibers.

To overcome these, chemical, physical and biological treatments are done, which include silane, acetone, and alkali treatment (Mohammadi *et al.* 2024, Li *et al.* 2007). Among the many flax fibers as reinforcement in composites, it has gained popularity in automotive applications in recent years (Bax and Muussig 2008, Skosana *et al.* 2025). Composites made of flax fibers with thermoplastic, thermoset, and biodegradable matrices have exhibited good mechanical properties compared to other natural fibers. Hence a green composite with flax as fiber reinforcement is considered for this work.

Researchers have reported that the mechanical properties of natural fibers and, thereby, matrix fiber adhesion can be improved by chemical treatment (Goriparthi *et al.* 2012, Goda *et al.* 2024). The most preferred chemical treatment is the alkali treatment using sodium hydroxide (NaOH) or potassium hydroxide (KOH), which will modify the structure and fiber surface. For this, the natural fibers are soaked in a known concentration of NaOH or KOH solution for a specific time. The hydroxyl group of fibers is eliminated as it reacts with NaOH to produce water molecules (H-OH). Further, Na-O combines with the cell wall of fiber to produce fiber cell-O-Na groups. Here flax fibers identified as fiber reinforcement, are treated with 2% NaOH solution at room temperature for 2 hours (Mabrouk *et al.* 2024, Chandrasekar *et al.* 2017). After the stipulated time, the flax fiber reinforcement is washed with deionized water to remove NaOH from fibers until the pH value is around 7. Later the fibers are dried for 24 hours (Maguteeswaran *et al.* 2024, Yan *et al.* 2012). This process will not only increase the mechanical properties but also remove its surface impurities and increase its adhesion properties. Effects of alkali treatments on bio composites are reported in detail (Sahu and Gupta 2020, Pokhriyal *et al.* 2024).

Plasticizers are added to the green composite to improve the brittleness and low impact resistance of PLA, which is used as resin in the composite (Al-Mulla *et al.* 2010). Plasticizers like epoxidized soybean oil methyl ester (ESOME) undergoes fast biodegradation when it is blended with PLA, and results an improvement in brittleness of industrial composting settings (Zych *et al.* 2021). Research has shown Epoxidized palm oil (EPO) is an epoxidized derivative of a mixture of esters of glycerol with various saturated and unsaturated fatty acids, will improve thermal stability and enhancement of ductility and flexibility for PLA/EPO blended composites (Ali *et al.* 2016, Kumar and Krishnan 2021).

Srinivas, Ananthapadmanabha *et al.* (2025), Sharma *et al.* (2019), Valapa *et al.* (2015) have reported that adding nano fillers has improved mechanical properties considerably. Graphene provides excellent functional properties by combining the layered structure of clays with the superior mechanical and thermal properties of carbon nanotubes (El Aoud *et al.* 2024, Sharma *et al.* 2019,

Valapa *et al.* 2015). The addition of 1% graphene nanoparticles in the PLA/EPO blend has increased the tensile strength by 26% and impact strength by 73% (Chieng *et al.* 2012). Influence of number of layers of braided flax fabric and loading along warp and weft directions on mechanical properties are reported (Kanakannavar and Pitchaimani 2022, Vasile *et al.* 2024). Hence a green composite made of flax fiber fabric as reinforcement material with PLA as the resin has been manufactured and tested for its mechanical properties, and the influence of matrix fillers such as EPO, graphene nanoparticles are studied are reported.

2. Methodology

2.1 Materials

Poly(lactic acid) (PLA) (Grade-3052D) used for matrix was purchased from Nature Tec India Pvt. Ltd Chennai, Tamil Nadu, India. The PLA had density of 1.24 g/cm³ and melting point 190 °C, as per supplier specification. The flax fiber in the form of balanced bidirectional woven fabric 0°/90° with 350 gsm was supplied by DLS Traders, Salem, Tamil Nadu, India. So obtained flax fibers were chemically treated as reported in L. Yan, N. Chou, and X. Yuan 2012. The graphene nano powder with outer diameter 10-20 micron and thickness 3-6nm with purity of 96-99% was purchased from United Nanotech Innovations, Bengaluru, Karnataka, India. The Epoxidized Palm Oil (EPO) was prepared in the Advanced Tribology Lab, College of Engineering Trivandrum, Kerala, India. Teflon sheet of thickness 0.5mm to prevent adhering of composite to the mould was supplied by vendor from Bangalore, Karnataka, India. Chloroform with a concentration of 99% used as the solvent and Sodium Hydroxide (NaOH) used for chemical treatment were supplied by Nice Chemicals Private Ltd, Kochi, Kerala, India. Mould with dimensions 310x260x4mm (Mild Steel Plates) for hot compressing the composites and Mild Steel Trays of dimensions 310x260x20mm for prepreg preparation were fabricated at Government Engineering College, Barton Hill, Thiruvananthapuram, Kerala, India.

2.2 Preparation of Epoxidized palm oil (EPO)

The basic principle of the epoxidation reaction of palm oil is illustrated schematically in Fig.1. The carbon-carbon double bonds present in the unsaturated fatty acid chains of palm oil react with peroxy acids to form epoxy (oxirane) groups, resulting in epoxidized palm oil (EPO). In the present study, epoxidation was carried out by initially mixing 100 mL of refined palm oil with 5 mL of acetic acid and 3-4 drops of concentrated sulfuric acid (H₂SO₄) as a catalyst. The mixture was manually swirled to ensure uniform mixing, after which the required quantity of hydrogen peroxide (H₂O₂) was added dropwise under a closed atmospheric condition to generate peracetic acid in situ. The reaction mixture was then subjected to constant magnetic stirring and heated at 70 ± 5°C for 4.5 h to facilitate the epoxidation of the unsaturated bonds. Upon completion of the reaction, the mixture was transferred to a separating funnel, where phase separation occurred, forming a clear aqueous layer at the bottom. This lower layer, containing unreacted reagents and by-products, was carefully removed. The epoxidized palm oil collected in the upper layer was subsequently washed five times with hot deionized water maintained at approximately 70°C to eliminate residual acids and oxidizing agents. Finally, the washed oil was dried using an electric heater coupled with a vacuum pump to remove traces of moisture, yielding the final epoxidized palm oil (EPO).

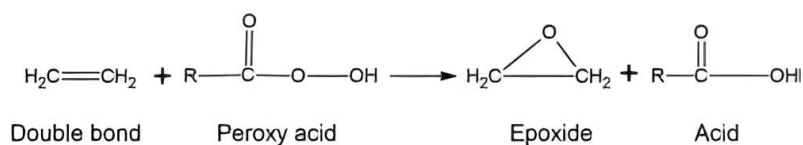


Fig. 1 Epoxidation reaction process

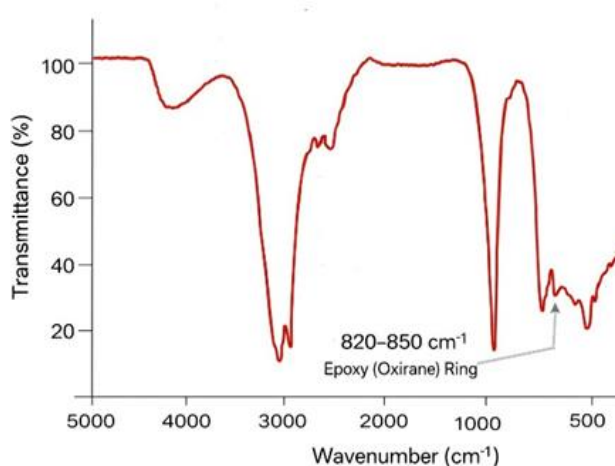


Fig. 2 FTIR spectrum of EPO

2.3 FTIR Analysis of EPO

Fig. 2 is the FTIR spectrum of epoxidized palm oil (EPO), which clearly confirms the successful epoxidation process performed on palm oil. The presence of prominent absorption peaks at about 2922 cm^{-1} and 2853 cm^{-1} can be assigned to the asymmetric and symmetric stretching vibrations of the aliphatic $-\text{CH}_2$ group, which suggests the intact structure of the hydrocarbon backbone in the fatty acid chains even after the epoxidation reaction. A prominent peak at about 1740 cm^{-1} can be assigned to the ester $\text{C}=\text{O}$ stretching vibration of triglycerides. The olefinic $\text{C}=\text{C}-\text{H}$ stretching band at about 3006 cm^{-1} is greatly reduced in intensity, indicating the effective utilization of the carbon-carbon double bounds in the epoxidation process. More importantly, the occurrence of a distinct absorption peak within the region of $820\text{--}850\text{ cm}^{-1}$ due to the epoxy (oxirane) ring vibration offers conclusive proof of the presence of epoxy functionality in the palm oil molecule. Moreover, the observed absorption band at about 1250 cm^{-1} corresponds to the $\text{C}-\text{O}-\text{C}$ stretching vibration of the epoxy functionality, indicating the efficacy of the epoxidation process. All these spectral features serve to collectively verify the process of converting palm oil into epoxidized palm oil and thereby justify its use as an ideal bio-based plasticizer and modifier for PLA composite materials.

2.4 Solvent Casting

In solvent casting process shown in Fig. 3, thermoplastic polymer films are formed by dissolving the polymer in a solvent, and this solution is used to form a film of the desired shape by using a mould. The polymer and solvent are the main components of this system, but additives are also

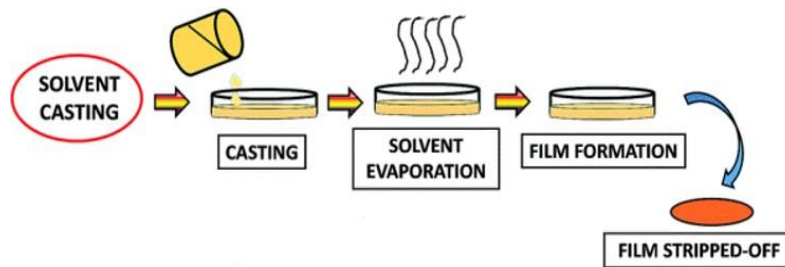


Fig. 3 Solvent Casting (Goriparthi *et al.* 2012)

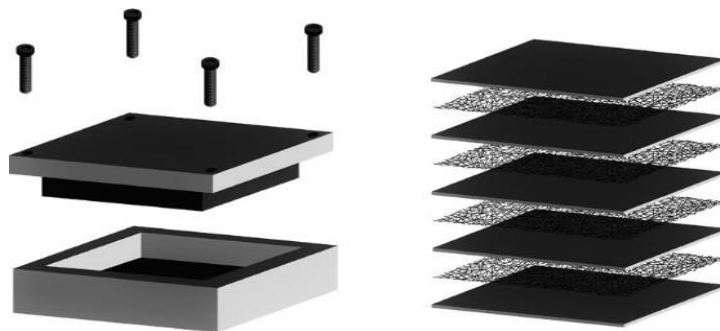


Fig. 4 Laminate Preparation

added. The main advantages of this method are better uniformity in the thickness of layers, good flexibility, and better physical properties. As reported (Goriparthi *et al.* 2012), the strength of the composite is improved after the solution casting due to the improvement in fiber impregnation and wettability. Moreover, the lack of thermal distortion maintains the fiber strength at higher values.

2.5 Hot Press Compression Moulding Method

In this process (Fig. 4), the preheated moulding material above the melting point, formed and cooled in the form of sheets, are kept open in a preheated mould cavity.

This material is compressed for a known pressure after closing the mould with a top member. Here, it is made sure that the applied pressure is uniformly distributed to all areas until the moulding material has cured, compression moulding. In this process, the design parameters are the moulding time, temperature, and pressure (Hasan *et al.* 2015).

2.6 Fabrication of Composite Laminates

The composite laminates were fabricated with a constant flax fiber fabric content of 30 wt.%. The remaining 70 wt.% comprised the PLA-based matrix, which was selectively modified by the addition of 5 wt.% EPO and 0.5 wt.% graphene nanoparticles (with respect to the matrix weight) in laminate 3. All laminate configurations were produced with the same flax fiber reinforcement weight fraction, and the observed differences in properties arise solely from variations in the matrix constituents. The fabrication of three different type of composite laminates shown in Table 1 are explained below.

Table 1 Types of Laminates

Sl. No.	Laminate	Combinations
1	Laminate 1 (L1)	PLA/Flax fiber fabric
2	Laminate 2 (L2)	PLA/Flax fiber fabric with EPO
3	Laminate 3 (L3)	PLA/Flax fiber fabric with EPO & Graphene nano particles



Fig. 5 PLA/Flax Composite Preparation; (a) PLA-Chloroform solution; (b) PrePreg Preparation; (c) Prepreg sheets after drying; (d) Specimens for Testing

2.6.1 PLA-Flax Composite

Green composites are manufactured by solution casting technique by dissolving PLA pellets in chloroform (solvent) in the ratio 10:1(v/w) and hot compressed, shown in Fig. 5. Here PLA sheets are prepared by dissolving PLA pellets in a known volume (1L) of chloroform by properly stirring for a known time (2 hrs.) and poured into an MS tray of dimensions 310x260x20 mm. These PLA sheets are allowed to cure by keeping them open for 24 hours at room temperature, and any chloroform present will evaporate. Similarly, Flax fiber/PLA sheets are prepared by pouring PLA/chloroform solution into another MS tray of the same dimensions. On the PLA/chloroform solution, Flax fiber fabric of size 310x260 mm was kept and above this fabric, poured a small amount of PLA/chloroform solution and this was also left for evaporation of chloroform for 24 hours. Likewise, five layers of PLA and four layers of Flax fiber/PLA prepreg sheets were prepared. A decrease in composite performance with an increase in temperature (from 230 °C to 250 °C) and process time (from 2–5 min) was reported (Bourmaud *et al.* 2020). Here these overlapped sheets are hot compressed at a pressure of 5 MPa at 180°C temperature for 15 minutes and later allowed to cure by keeping it at room temperature for 6 hours. After curing, these samples are made to ASTM testing standards. Teflon sheets and silicon grease were used to avoid sticking the matrix in the mould during hot compression. The density of the fabricated Laminate 1 was measured using the Archimedes principle, and the resulting density was found to be 1.15 g/cm³.

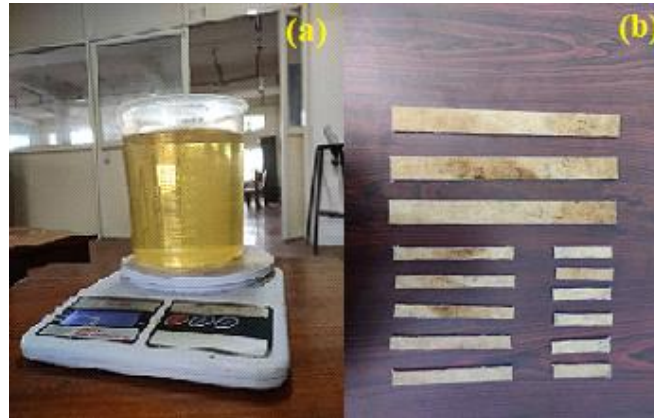


Fig. 6 PLA-EPO/Flax Composite Preparation; (a) PLA-EPO/Chloroform Solution; (b) Prepared Specimens

2.6.2 PLA-Flax Composite with EPO

A known amount of PLA pellets and chloroform solvent were taken in a volume beaker in the ratio 10:1(v/w). The PLA gets dissolved in the chloroform on stirring over a mechanical stirrer for about 2 hours at a slow speed. After the solubilization of PLA, about 5 wt% EPO was added and stirred for another 1 hour to form a better PLA/EPO blend solution. The same methodology used for manufacturing PLA-Flax Composite is also used here for PLA-Flax Composite with EPO shown in Fig. 6. The density of the fabricated Laminate 2 was measured, and the resulting density was found to be 1.12 g/cm³.

2.6.3 PLA-Flax Composite with EPO and Graphene Nano filler

A known amount of PLA pellets were dissolved in the chloroform solvent taken in a volume beaker in the ratio 10:1 (v/w). The PLA gets dissolved in the chloroform on stirring over a mechanical stirrer for about 2 hours (Porrás and Marañón 2012).

After the solubilization of PLA, EPO of about 5 wt% was added and stirred for another 1 hour to form a better PLA/EPO blend solution. At the same time, 0.5% graphene powder was added to 20 ml chloroform and ultrasonicated in an ice-water bath for 30 minutes. The graphene/Chloroform solution is then added drop by drop into the PLA-EPO/Chloroform solution and is stirred for a period of 1 hour. Followed by this, PLA-EPO-graphene blend films were prepared by pouring a small amount of PLA-EPO-graphene/chloroform solution into an MS tray. The setup was then kept for 24 hours at room temperature to evaporate chloroform.

At the same time, Flax/PLA-EPO-graphene blend films were prepared by pouring PLA-EPO-graphene/chloroform solution into another MS tray. On the PLA-EPO-graphene/chloroform solution, Flax fabric of size 310x260mm was kept. Above this fabric, again, a small amount of PLA-EPO-graphene/chloroform solution was poured, and this was also left for evaporation of chloroform for 24 hours. Likewise, five layers of PLA-EPO-graphene sheets were prepared, and four layers of Flax/PLA-EPO- graphene prepreg sheets were also prepared. The sheets were stacked alternatively inside the mould, and this arrangement was placed in the hot compression moulding machine. Then compression was done with a pressure of 5 MPa applied at 180°C temperature for 15 minutes, and the composite laminate was left for cooling at room temperature for 6 hours. After cooling, different test samples were cut according to ASTM testing standards as shown in Fig. 7. Teflon sheets and



Fig. 7 PLA-Flax fiber with EPO and Graphene Composite Preparation; (a) PLA-EPO-Graphene solution; (b) PrePrep Preparation; (c) Prepreg sheets after drying; (d) Specimens for Testing

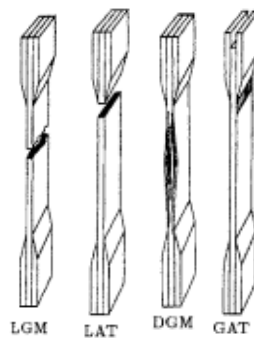


Fig. 8 Tensile test failure modes/codes (ASTM D3039, 2008)

silicon grease were used to avoid sticking the matrix in the mould during hot compression. The density of the fabricated Laminate 3 was measured, and the resulting density was found to be 1.26 g/cm^3 .

2.7 Mechanical Characterization of Composites

2.7.1 Tensile Test

The laminates' tensile strength was measured using the ASTM D3039 standard. The specimen is loaded in such a manner that the breakage should occur in the expected region and its necessity depends on the localization of the breakage. Mechanics behind the composite failure modes are explained in detail (Jones 1975). The important three-part failure mode codes as per ASTM definitions are given in Fig. 8. The specimen dimensions were taken as $250 \times 25 \times 4 \text{ mm}$. The ends of

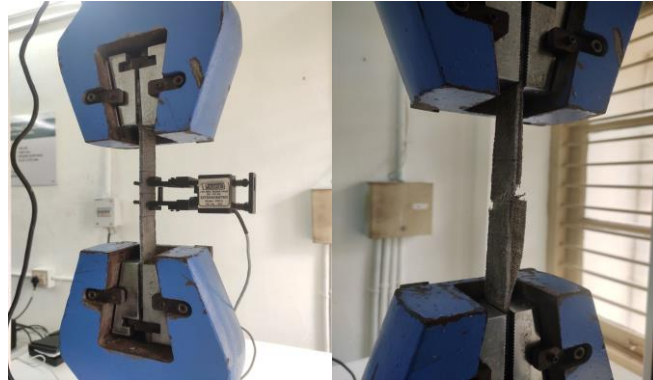


Fig. 9 Tensile test specimen with the experimental setup

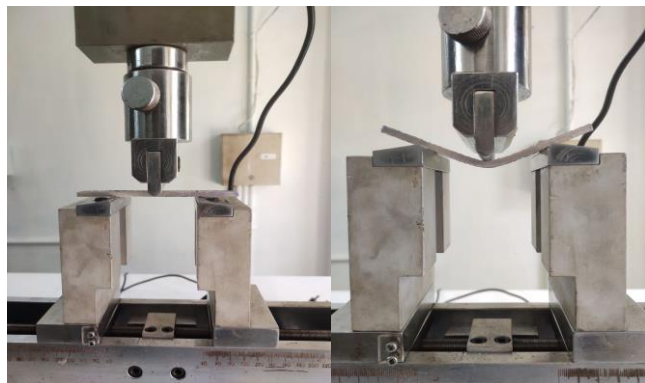


Fig. 10 Flexural test specimen with the experimental setup

the specimen were clamped between the jaws. The tensile velocity used during the tensile test was 5 mm/min, in accordance with ASTM D3039 standards for polymer matrix composites.

The movement of the jaw offers tensile force on the specimen. This force was recorded with respect to the change in gauge length. The tensile test was done on Computerized Universal Testing Machine (Make: KALPAK UTM, Model No. KIC-2-1000-C with a maximum load capacity of 100 kN). The samples were tested at a loading rate of 5 mm/min. The specimen, which was cut from three different types of laminates, was subjected to a tensile test for five samples per laminate to get an average value. The tensile test specimens with experimental setup of various laminates are shown in Fig. 9. Many researchers (Sakhivel and Ramesh 2013, Alavudeen *et al.* 2011) showed that stacking sequence plays significant role in determining the tensile properties of the composite. The factors that influence the tensile response are materials used, methods of material Preparation, fiber layer stacking sequence, specimen preparation, specimen conditioning, the environment of testing, speed of testing, void content and most importantly the fiber weight fraction. The extensometer used here has a gauge length of 25 mm.

2.7.2 Flexural Test

The force required to bend the specimen along the middle has been measured by imposing both tensile and compressive stresses on both sides of the specimen. The test was performed on the



Fig. 11 Izod impact specimen with the experimental setup

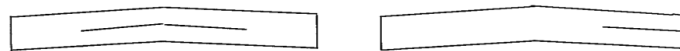


Fig. 12 Typical failure mode in the short beam test (ASTM D 2344, 2006)

Computerized Universal Testing Machine (Make: KALPAK UTM, Model No. KIC-2-1000-C with a maximum load capacity of 100 kN)). The specimens prepared were of size 127 x 12.7 x 4 mm based on the ASTM D790 test standard, and the span length was taken as standard as 64 mm in the ratio of 16:1 as per ASTM D 790.

Three-point bending test was performed with an applied load of 2 mm/min until the specimen fractures and broke. The experimental set up of flexural test specimen before and after bending is shown in Fig. 10. Here in the test specimen, both compressive and tensile stress will be acting simultaneously. The maximum load is recorded either when the maximum strain reaches 0.05 mm/min or at specimen failure; from the recorded maximum load, the values for modulus of elasticity.

2.7.3 Impact Test

The specimens of size 64x12.7x4 mm conforming to ASTM D256 standard are tested for impact strength using an Izod impact test rig; from the impact made by the pendulum on the specimen, the impact energy required for crack initiation to the same for breakage of the specimen is plotted. Fig. 11 shows the test specimens with set up used for the Izod impact test.

2.7.4 Short Beam Test

Unlike other materials, the complex structure of composites makes the internal stress nature also complicated. Here the matrix, the resin, and interlaminar properties have a critical role to play in the failure modes. Here a small ratio of width to span (1:3) as per ASTM D2344 has been taken for performing the ILSS test. The failure modes in this test method are shown in Fig. 12.

The interlaminar shear strength (Short beam strength) is obtained by using the expression.

$$F_{sbs} = 0.75 \frac{p}{bh} (\text{MPa})$$

where p = maximum Load observed during the test (N), b = width (mm), h = thickness (mm)

The ILSS specimens with experimental setup are shown in Fig. 13.



Fig. 13 ILSS specimen with the experimental setup

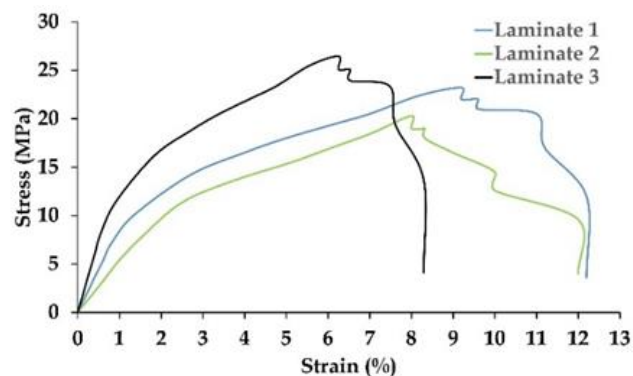


Fig. 14 Stress Vs % Strain variation of composite laminates

2.7.5 Scanning Electron Microscopy

The fracture surfaces of tensile test specimens of PLA/Flax fabric, PLA/EPO Flax fabric and PLA/EPO/Graphene Flax fabric specimens were observed by scanning electron microscopy (SEM) of model TESCAN VEGA 3 LMU high-performance, Variable Pressure Analytical SEM with LAB6 having high resolution of 2 nm, along with the most advanced LN₂-free high-resolution. Prior to the analysis, the specimens were coated with a thin layer of gold to get good conductivity, using a Quorum SC7620 sputter coater.

3. Results and Discussion

3.1 Tensile Properties

A detailed study of flax fiber-based composites with different combinations was carried out for this, and three laminates were prepared as shown in Table 1. The tensile properties of the laminates were measured by using the ASTM D3039 standard. In this study, as mentioned earlier, a Computerized Universal Testing Machine (Make: KALPAK UTM, Model No. KIC-2-1000-C with a maximum load capacity of 100 kN). The specimen clamped is of dimension 250x25x4 mm, and the ends of the specimen have been clamped between the jaws so that the breakage is occurring in

Table 2 Mechanical Properties of Flax Fiber Reinforced Composites (Experimental results)

Laminate	Tensile Strength (MPa)	Tensile Modulus (GPa)	Flexural Strength (MPa)	Flexural Modulus (GPa)	Impact Energy (J/m)	Short Beam Strength (MPa)
L1	23.20 ± 1.12	2.55 ± 0.14	121.86 ± 5.23	2.90 ± 0.18	40.35 ± 2.05	31.25 ± 1.75
L2	20.30 ± 0.95	1.25 ± 0.08	90.35 ± 4.10	1.30 ± 0.12	33.58 ± 1.85	21.65 ± 1.30
L3	26.45 ± 1.30	3.20 ± 0.20	132.56 ± 6.10	3.80 ± 0.25	43.69 ± 2.20	35.85 ± 2.05

the expected region. The tensile force on the specimen was recorded with respect to the change in gauge length at a loading rate of 5 mm/min. The specimen, which was cut from three different types of laminates, was subjected to a tensile test for five samples per laminate to get an average value, and are shown in Table 2.

The extensometer used here has a gauge length of 25 mm, and the values obtained for induced stress and % strain are plotted and shown in Fig. 14. The initial linear portion of the curve accounted for the elastic behavior, and the variation from the linear portion is due to the initiation of a crack in the matrix and also accounted for the start of fiber failure.

As the loading continued, the crack also propagated, leading to the failure of fracture of fiber and resulting in fiber failure; the value corresponds to ultimate stress. The ultimate stress value obtained for laminate 1 composite is 23.20 MPa, which is high for the same combination composite for fiber 18.80 MPa as reported in the literature (Kumar and Krishnan 2021). The ultimate stress value is attributed to the increased strength due to the interlocking effect of the woven structure of the fabric (Girones *et al.* 2011). The polar oxygen atoms present in the Poly Lactic Acid (PLA), used as the resin here, react to the hydroxyl groups in the flax fiber to form hydrogen bonds, which in turn create strong bonding (Goriparthi *et al.* 2012). Some studies reported that non-woven natural fiber reinforced composites provides lesser tensile strength as compared to woven mats (Yongli Zhang *et al.* 2013). Even though a wide range of values starts from 21 MPa (Nishino *et al.* 2013) to 110 MPa (Shibata *et al.* 2003) for tensile strength for the laminate 1 composites has been reported, the value obtained as shown in Table 2 for the same composition here of 23.20 MPa falls within the range, also an observed value of 2.55 GPa for Young's Modulus, hence the test procedure is justified. Even though the laminate 1 has high strength but it is highly brittle due to the presence of PLA; furthermore, laminate 1 is of slow degradation rate.

In order to overcome these limitations, laminate 2 was prepared by adding 5% EPO to laminate 1. Anis Nazurah Mohd Nasir *et al.* (2016) has reported that the addition of chemical reaction epoxidized palm oil (EPO) in rubber composites, has increased mechanical properties, including lowering of brittle nature. Laminate 2 was tested to tensile strength, and the value was found to be 20.30 MPa and Young's modulus value of 1.25 GPa. Even though the tensile strength and Young's modulus values were found to be less when compared with laminate 1, there has been a considerable increase in the ductility of the composite. It was also noted that there is a change in viscosity due to the addition of EPO contributes to the laminate being more flexible.

Even though the ductility of composite has increased considerably in laminate 2 by the addition of EPO but only with a compromise to the tensile strength, which reduces the industry application range; hence the strength needs to be enhanced. For this 0.5 % graphene has been added to the laminate 2 combinations, hence laminate 3. A tensile test was carried out for laminate 3, and the results were plotted. It is seen that there is a considerable increase in the mechanical properties of

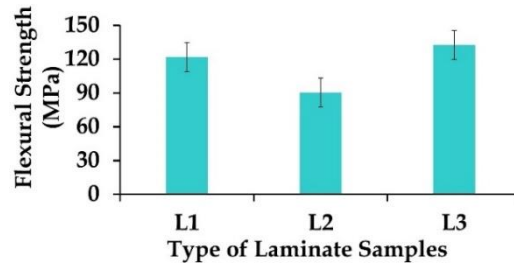


Fig. 15 Plot of Flexural stress variation of different laminate

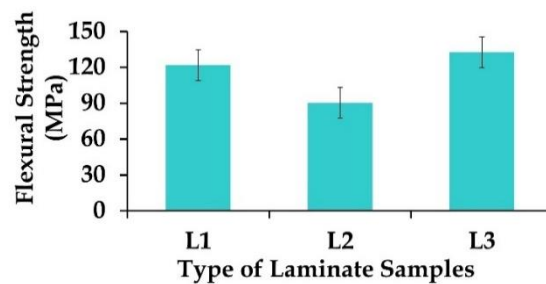


Fig. 16 Plot of Flexural Modulus variation of laminates

laminate 3, especially in the case of tensile strength. For laminate 3 the maximum tensile strength value obtained is 26.45 MPa, and Young's modulus value of 3.20 GPa. The reason for this is attributed to the better dispersion and spread of the graphene nanoparticle (Valapa *et al.* 2015); for this, SEM images were taken, and analysis will be followed in a later section. In short, from the tensile test results, it is evident that by the addition of EPO, there was a significant increase in ductility at the expense of tensile strength, as seen in laminate 2, which was compensated by the addition of graphene.

In terms of tensile behavior, the higher density (1.26 g/cm^3) of laminate 3 enabled efficient stress transfer across the fiber–matrix interface, resulting in the highest tensile strength ($\sim 26 \text{ MPa}$). Conversely, the lower density of L2 reflects increased free volume due to EPO plasticization, which reduced tensile load-bearing capacity despite improved ductility.

3.2 Flexural Properties

Similar to the tensile test three-point bending test for laminates was carried out in Computerized Universal Testing Machine (Make: KALPAK UTM, Model No. KIC-2-1000-C with a maximum load capacity of 100 kN) as per ASTM test standard D 790-10. Owing to the bending theory, the strain rate for the outer layer of the laminates was tested in displacement control mode at a constant crosshead speed of 5 mm/min. The span length for the three-point flexural test was selected as 64 mm according to the specimen thickness.

The results obtained for the flexural test are recorded in Table 2, and it is seen that flexural strength values follow the same trend as that of the tensile test. The current study showed that the fabricated composite possesses enough flexural strength for this application. A graph with variation of flexural stress and modulus was also plotted, as shown in Figs. 15-16.

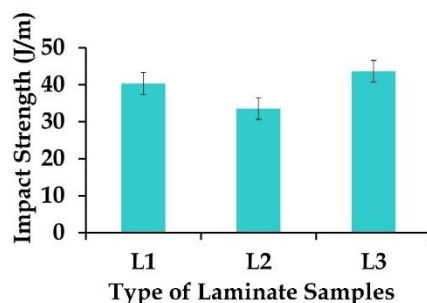


Fig. 17 Plot of variation of Impact strength of laminates

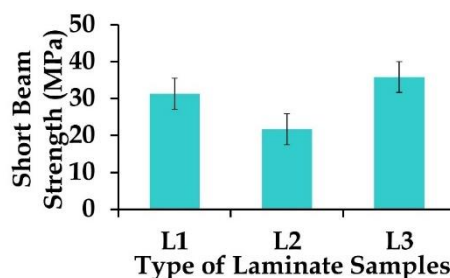


Fig. 18 Inter laminar short beam shear strength for different laminates

During the test, no specimen has failed by delamination, and the failure mode shows little or no fiber pull-out. The crack always initiates on the tension side of the beam, and the fracture was observed in the middle of the specimen. Normally, the modulus is very susceptible to the matrix/fiber interfacial bonding. Average values for the ultimate flexural strength and flexural modulus for the laminate 1 are 121.86 MPa and 2.9 GPa, respectively, and corresponding values for the laminates 2 and 3 are 90.35 MPa, 1.3 GPa, and 132.56 MPa, 3.8 GPa respectively, shown in Table 2.

For flexural strength, laminate 3 demonstrated the maximum value of 132.56 MPa, which is attributed to its dense (1.26 g/cm³) and rigid structure that effectively resisted bending deformation. The reduced density of laminate 2 (1.12 g/cm³) led to significant loss in flexural strength (90.35 MPa), while laminate 1 (1.15 g/cm³) showed intermediate performance corresponding to its moderate density.

3.3 Impact Properties

The specimens of laminates 1, 2 & 3 conforming to ASTM D256 standard dimensions were tested for impact strength using an Izod impact test rig and are plotted in Fig. 17.

The average impact strength obtained as shown in Table 2 from laminate 1, 2, and 3 is 40.35 J/m, 33.58 J/m, and 43.69 J/m, respectively. The results show the same pattern as that of the tensile test and flexural test conducted. The impact strength value of 40.35 J/m for laminate 1 is in line with the literature. The reduction in impact for value for laminate 2 is attributed to the propagation of the EPO into the matrix structure and the presence in the interfacial area and also due to the intermolecular interaction caused by the PLA. In comparison, the better dispersion and spread of the graphene nanoparticle attribute for the increase in impact strength values for laminate 3. The impact

Table 3 Comparative evaluation of mechanical properties of PMCs

Composite System	Tensile Strength (MPa)	Flexural Strength (MPa)	Impact Strength (J/m)	Source
PLA/Flax	~50–350 MPa	~60–360 MPa	~600–800	(Sanivada <i>et al.</i> 2020, Sundeep <i>et al.</i> 2022)
Flax/PP	~30–58 MPa	~53–67 MPa	~25–46 kJ/m ²	(Sayeed <i>et al.</i> 2023)
Flax/PP (~30 wt%)	~25–48	~15–38	—	(Wu <i>et al.</i> 2016)
Flax/ β -PP	~25–38 MPa	~15.5–37.8 MPa	N/A	(Wu <i>et al.</i> 2016)
PLA/flax (UD, ~30 wt%)	~177	~215	—	(Sanivada <i>et al.</i> 2020)
GF/PP	~200–300+ MPa	~300–400+ MPa	High	(Li <i>et al.</i> 2024)
Epoxy/GF	~227–278 MPa	~225	N/A	(Couture <i>et al.</i> 2016)
PLA/Flax fiber fabric with EPO & Graphenenano particles	26.48	132.56	43.65	Present Study

strength of laminate 3 (43.69 J/m) benefited from its higher density (1.26 g/cm³), which facilitated better energy absorption and crack-arresting mechanisms through a combination of matrix toughness and graphene reinforcement. In contrast, the lower-density of laminate 2 (1.12 g/cm³) exhibited inferior impact resistance due to insufficient structural integrity.

3.4 Short Beam Test

The short beam test for determining the interlaminar shear strength of laminates was carried out using a three-point bending test, as mentioned in the previous section. The specimen made of laminates was aligned to ASTM D 2344-06 standards by keeping the ratio of length to thickness as 6:1 and width to thickness ratio as 2:1.

The values obtained as shown in Fig. 18 for short beam strength of laminates 1, 2, and 3 were 31.25 MPa, 21.65 MPa and 35.85 MPa respectively. Even though all the laminates failed during the test due to delamination, the short beam strength values obtained followed the same pattern as that of the tensile, flexural, and impact strength, with maximum value for short beam strength obtained for laminate 3 due to the even spread and better dispersion of graphite nanoparticles.

The summary of the mechanical properties obtained for all three laminates for various test are given in Table 2. The merit of the developed laminate 3 (PLA/flax fiber fabric with EPO and graphene nanoparticles) in terms of performance over current polymeric matrix composites used in automobiles will become clear from the following comparison (Table 3). Though the tensile strength of the developed composite (26.48 MPa) appears to be lower in comparison to high-performance composites GF/PP and epoxy/GF composites used as auto-mobile parts, still it matches with and also tends to fall within the range defined by flax/PP composites already being used in non-structural and semi-structural auto-mobile parts. It may further be noted that the flax/PP composite possesses a high value of Flexural strength of 132.56 MPa as against many flax/PP composites; still, its value tends to approach the lower limit of PLA/flax composites; this proves its high resistance against flexure and withstands bending loads with effectiveness. Moreover, the high value of Impact resistance of 43.65 J/m proves the efficient absorption of foreign bodies and their energies to desired levels; also matches with natural-fiber reinforced thermoplastics.

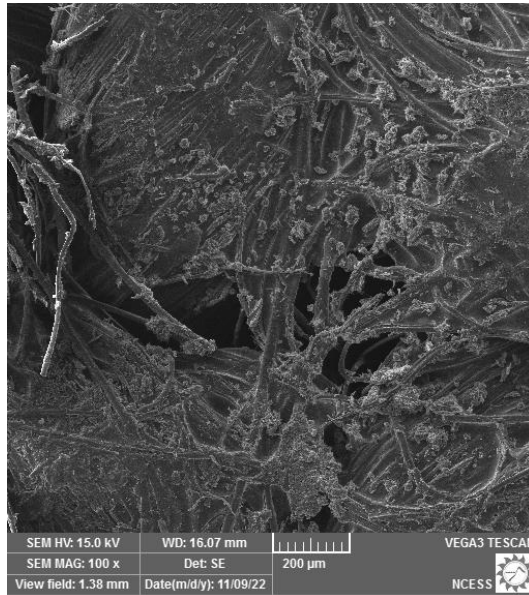


Fig. 19 Fractured surface of FLAX – PLA Laminate

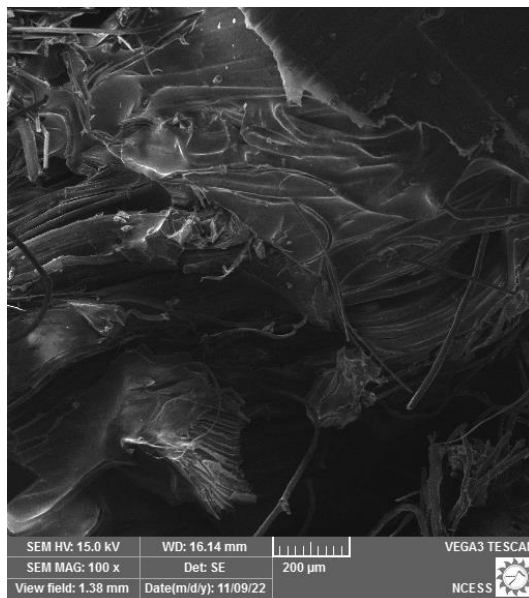


Fig. 20 Fractured surface of FLAX – PLA-EPO Laminate

3.5 Scanning Electron Microscopy (SEM) Analysis

SEM images to observe the surface morphology at the rupture part of the tensile samples of the laminates 1, 2, and 3 were taken and are shown in Figs. 19-21. All SEM micrographs presented in Figs. 18-20 were acquired using a VEGA3 TESCAN SEM under an accelerating voltage of 15 kV,

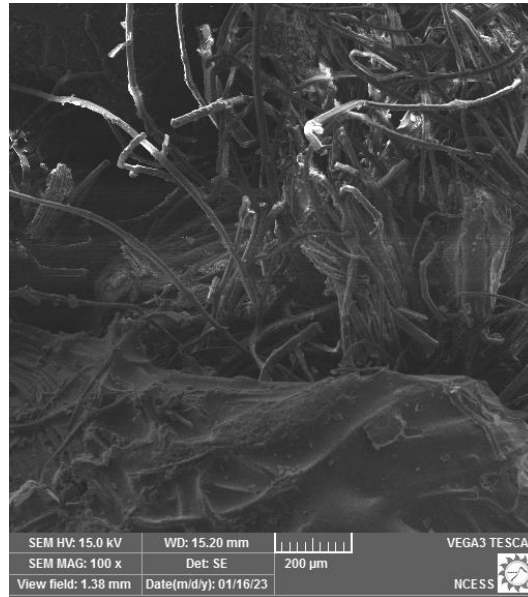


Fig. 20 Fractured Fig. 21 Fractured surface of FLAX - PLA – EPO-Graphene Laminate of FLAX – PLA-EPO Laminate

working distance of ~ 16 mm, and secondary electron (SE) detector. The images were captured at a magnification of $100\times$ with a scale bar of $200\ \mu\text{m}$ indicated in each figure.

The images show the damage caused to the matrix due to the tensile loading; it also shows the penetration of resin into the reinforcements and filling the voids, thereby creating good bonding between both. The presence of bundled fibers in the laminates 1 & 3 indicates good adhesion within the matrix and the fibers. The presence of micro voids in laminate 2 attributed to the reduction in strength, as reported in all the tests. However, the clear image of good dispersion with strong bonding between the layers of fibers and matrix shown in the laminate 3 supports the higher mechanical properties obtained in all the tests performed.

4. Conclusions

The incorporation of Epoxidized Palm Oil (EPO) and graphene nano fillers into PLA/flax fiber fabric composites significantly enhanced their mechanical performance, positioning them as promising biodegradable materials for automotive applications. Compared to the baseline Laminate 1 (PLA/flax), the addition of 5% EPO in Laminate 2 led to a slight reduction in tensile (-12.5%), flexural (-25.9%), and impact strength (-16.8%) due to the plasticizing effect of EPO, which improved flexibility but compromised overall strength. However, Laminate 3, which incorporated both EPO and 0.5% graphene nanoparticles, outperformed all others, demonstrating an impressive 13.9% increase in tensile strength, 8.8% increase in flexural strength, and 8.3% enhancement in impact strength compared to Laminate 1. These improvements highlight the synergistic effect of EPO and graphene, where EPO enhances ductility and graphene reinforces the composite matrix, leading to superior load-bearing capability and energy absorption. Thus, Laminate 3 emerges as the

most effective and eco-friendly solution, aligning with the pressing demand for sustainable materials in the automotive sector.

Acknowledgement

Author gratefully acknowledge the support of Machine Design section, Government Engineering College, Barton Hill, Thiruvananthapuram for allowed to use KALPAK Computerized UTM instrument to conduct testing and Hot Press Compression Moulding Machine at National Institute of Rubber Training (NIRT), Kottayam for their help in making biodegradable green composite laminates.

References

- Alavudeen, A., Thiruchitrambalam, M., Venkateshwaran, N. and Athijayamani, A. (2011), "Review of natural fiber reinforced woven composite", *Rev. Adv. Mater. Sci.*, **27**, 146-150
- Ali, F.B., Awale, R.J., Fakhrudin, H. and Anuar, H. (2016), "Plasticizing poly (lactic acid) using epoxidized palm oil for environmental friendly packaging material", *Malaysian J. Anal. Sci.*, **20**(5), 1153-1158. <http://doi.org/10.17576/mjas-2016-2005-22>
- Al-Mulla, E.A.J., Yunus, W.M.Z.W., Ibrahim, N.A.B. and Rahman, M.Z.A. (2010), "Properties of epoxidized palm oil plasticized poly(lactic acid)", *J. Mater. Sci.*, **45**, 1942-1946. <https://doi.org/10.1007/s10853-009-4185-1>
- Anis, N., Ahmad, Z.R. and Azizol, W. (2014), "Properties of epoxidised palm oil (EPO)/styrene butadiene rubber (SBR) compound", *Adv. Environ. Biol.*, **8**(8), 2589-2599.
- Bax, B. and Muessig, J. (2008), "Impact and tensile properties of PLA/Cordenka and PLA/flax composites", *Compos. Sci. Tech.*, **68**, 1601-607. <https://doi.org/10.1016/j.compscitech.2008.01.004>.
- Bourmaud, A., Shah, D.U., Beaugrand, J. and Dhakal, H.N. (2020), "Property changes in plant fibres during the processing of bio-based composites", *Ind. Crops Prod.*, **154**, 112705. <https://doi.org/10.1016/j.indcrop.2020.112705>
- Chandrasekar, M., Ishak, M.R., Sapuan, S.M., Leman, Z. and Jawaid, M. (2017), "A review on the characterisation of natural fibres and their composites after alkali treatment and water absorption", *Plast. Rubber Compos.*, **46**(3), 119-136. <https://doi.org/10.1080/14658011.2017.1298550>
- Chieng, B.W., Ibrahim, N.A., Yunus, W.M.Z.W., Hussein, M.Z. and Giita Silverajah, V.S. (2012), "Graphene nanoplatelets as novel reinforcement filler in poly (lactic acid)/epoxidized palm oil green nanocomposites: Mechanical properties", *Int. J. Mol. Sci.*, **13**(9), 10920-10934. <https://doi.org/10.3390/ijms130910920>
- Couture, A., Lebrun, G. and Laperrière, L. (2016), "Mechanical properties of polylactic acid (PLA) composites reinforced with unidirectional flax and flax-paper layers", *Compos. Struct.*, **154**, 286-295. <https://doi.org/10.1016/j.compstruct.2016.07.069>
- El Aoud, B., Althobaiti, S., Aljohani, A.F., Selim, M.M., Boujelbene, M., Mohamed, S.M. and Mahariq, I. (2024), "Micromechanical modeling of thermal conductivities of unidirectional carbon fiber/epoxy composites containing carbon nanotube/graphene hybrids", *Int. Commun. Heat Mass Transf.*, **157**, 107726.
- Farah, S., Anderson, D.G. and Langer, R. (2016), "Physical and mechanical properties of PLA, and their functions in widespread applications—A comprehensive review", *Adv. Drug Deliv. Rev.*, **107**, 367-392. <https://doi.org/10.1016/j.addr.2016.06.012>
- Gironès, J., Lopez, J.P., Vilaseca, F., Herrera-Franco, P.J. and Mutje, P. (2011), "Biocomposites from Musa textilis and polypropylene: Evaluation of flexural properties and impact strength", *Compos. Sci. Tech.*, **71**(2), 122-128. <https://doi.org/10.1016/j.compscitech.2010.10.012>
- Goda, I., Padayodi, E. and Raoelison, R.N. (2024), "Enhancing fiber/matrix interface adhesion in polymer composites: Mechanical characterization methods and progress in interface modification", *J. Compos.*

- Mater.*, **58**(29), 3077-3110. <https://doi.org/10.1177/00219983241283958>
- Goriparthi, B.K., Suman, K. and Rao, N.M. (2012), "Effect of fiber surface treatments on mechanical and abrasive wear performance of polylactide/jute composites", *Compos. Part A Appl. Sci. Manuf.*, **43**(10), 1800-1808. <https://doi.org/10.1016/j.compositesa.2012.05.007>
- Hasan, M., Hoque, M.E., Mir, S.S., Saba, N., Sapuan, S.M. (2015), "Manufacturing of Coir Fibre-Reinforced Polymer Composites by Hot Compression Technique", In: *Salit, M., Jawaid, M., Yusoff, N., Hoque, M. (eds) Manufacturing of Natural Fibre Reinforced Polymer Composites*. Springer, Cham. https://doi.org/10.1007/978-3-319-07944-8_15
- Islam, M.A., Islam, M.M., Yang, C., Wodag, A.F., Wang, R., Chen, W., Zhou, B., Gao, S. and Xu, F. (2024), "Development of three dimensional (3D) woven flax/PLA composites with high mechanical and thermal properties using braided yarns", *Ind. Crops Prod.*, **222**, 119580. <https://doi.org/10.1016/j.indcrop.2024.119580>
- Islam, T., Chaion, M.H., Jalil, M.A., Rafi, A.S., Mushtari, F., Dhar, A.K. and Hossain, S. (2024), "Advancements and challenges in natural fiber-reinforced hybrid composites: a comprehensive review", *SPE Polymers*, **5**(4), 481-506. <https://doi.org/10.1002/pls2.10145>
- Jones, R.M. (1999), *Mechanics of Composite Materials (2nd ed.)*, CRC Press, Florida, United States. <https://doi.org/10.1201/9781498711067>
- Kanakannavar, S. and Pitchaimani, J. (2022), "Fabrication and mechanical properties of braided flax fabric polylactic acid bio-composites", *J. Textile Inst.*, **113**(5), 833-845. <https://doi.org/10.1080/00405000.2021.1907958>
- Kandola, B.K., Mistik, S.I., Pornwannachai, W. and Anand, S.C. (2018), "Natural fibre-reinforced thermoplastic composites from woven-nonwoven textile preforms: Mechanical and fire performance study", *Compos. Part B Eng.*, **153**, 456-464. <https://doi.org/10.1016/j.compositesb.2018.09.013>
- Li, J., Sun, Y., Zhang, B. and Qi, G. (2024), "Mechanical, dielectric and flame-retardant properties of GF/PP modified with different flame retardants", *Polymers*, **16**(12), 1681. <https://doi.org/10.3390/polym16121681>
- Li, X., Tabil, L.G. and Panigrahi, S. (2007), "Chemical treatments of natural fiber for use in natural fiber-reinforced composites: a review", *J. Polym. Environ.*, **15**, 25-33. <https://doi.org/10.1007/s10924-006-0042-3>
- Liu, W., Chen, T., Fei, M.E., Qiu, R., Yu, D., Fu, T. and Qiu, J. (2019), "Properties of natural fiber-reinforced biobased thermoset biocomposites: Effects of fiber type and resin composition", *Compos. Part B Eng.*, **171**, 87-95. <https://doi.org/10.1016/j.compositesb.2019.04.048>
- Mabrouk, O.M., Khair-Eldeen, W., Hassanin, A.H. and Hassan, M.A. (2024), "The influence of alkaline treatment on delamination resistance of woven flax fiber-reinforced epoxy composite laminates", *Fiber. Polym.*, **25**(12), 4859-4872. <https://doi.org/10.1007/s12221-024-00747-6>
- Maguteeswaran, R., Prathap, P., Satheeshkumar, S. and Madhu, S. (2024), "Effect of alkali treatment on novel natural fiber extracted from the stem of Lankaran acacia for polymer composite applications", *Biomass Convers. Biorefin.*, **14**(6), 8091-8101. <https://doi.org/10.1007/s13399-023-04189-7>
- McClements, D.J. (2024), "Composite hydrogels assembled from food-grade biopolymers: Fabrication, properties, and applications", *Adv. Colloid Interf. Sci.*, **332**, 103278. <https://doi.org/10.1016/j.cis.2024.103278>
- Mohammadi, M., Ishak, M.R. and Sultan, M.T.H. (2024), "Exploring chemical and physical advancements in surface modification techniques of natural fiber reinforced composite: a comprehensive review", *J. Natural Fiber.*, **21**(1), 2408633. <https://doi.org/10.1080/15440478.2024.2408633>
- Nishino, T., Hirao, K., Kotera, M., Nakamae, K. and Inagaki, H. (2003), "Kenaf reinforced biodegradable composite", *Compos. Sci. Tech.*, **63**(9), 1281-1286. [https://doi.org/10.1016/S0266-3538\(03\)00099-X](https://doi.org/10.1016/S0266-3538(03)00099-X)
- Nurul Fazita, M.R., Jayaraman, K., Bhattacharyya, D., Mohamad Haafiz, M.K., Saurabh, C.K., Hussin, M.H. and HPS, A.K. (2016) "Green composites made of bamboo fabric and poly (lactic) acid for packaging applications—a review", *Materials*, **9**, 435 <https://doi.org/10.3390/ma9060435>
- Parameswaranpillai, J., Rangappa, S.M., Siengchin, S. and Jose, S. (Eds.). (2021), *Bio-based Epoxy Polymers, Blends, and Composites: Synthesis, Properties, Characterization, and Applications*. John Wiley & Sons,

- Weinheim.
- Pickering, K. (2008), *Properties and Performance of Natural-Fibre Composites*, Woodhead Publishing, Cambridge, England.
- Pokhriyal, M., Rakesh, P.K., Rangappa, S.M. and Siengchin, S. (2024), "Effect of alkali treatment on novel natural fiber extracted from *Himalayacalamus falconeri* culms for polymer composite applications", *Biomass Convers. Biorefin.*, **14**(16), 18481-18497. <https://doi.org/10.1007/s13399-023-03843-4>
- Porras, A. and Maranon, A. (2012), "Development and characterization of a laminate composite material from polylactic acid (PLA) and woven bamboo fabric", *Compos. Part B Eng.*, **43**(7), 2782-2788. <https://doi.org/10.1016/j.compositesb.2012.04.039>
- Sahu, P. and Gupta, M.K. (2020), "A review on the properties of natural fibres and its bio-composites: Effect of alkali treatment", *Proceedings of the Institution of Mechanical Engineers, Part L: Journal of Materials: Design and Applications*, **234**(1), 198-217. <https://doi.org/10.1177/1464420719875163>
- Sakthivel, M. and Ramesh, S. (2013), "Mechanical properties of natural fibre (banana, coir, sisal) polymer composites", *Sci. Park*, **1**(1), 1-6.
- Sangeetha, V.H., Deka, H., Varghese, T.O. and Nayak, S.K. (2018), "State of the art and future prospectives of poly (lactic acid) based blends and composites", *Polym. Compos.*, **39**(1), 81-101. <https://doi.org/10.1002/pc.23906>
- Sanivada, U.K., Mármol, G., Brito, F.P. and Figueiro, R. (2020), "PLA Composites Reinforced with Flax and Jute Fibers-A Review of Recent Trends, Processing Parameters and Mechanical Properties", *Polymers*, **12**(10). <https://doi.org/10.3390/polym12102373>
- Sayeed, M.A., Sayem, A.S.M., Haider, J., Akter, S., Habib, M.M., Rahman, H. and Shahinur, S. (2023), "Assessing mechanical properties of jute, kenaf, and pineapple leaf fiber-reinforced polypropylene composites: experiment and modelling", *Polymers*, **15**(4). <https://doi.org/10.3390/polym15040830>
- Sharma, S., Singh, A.A., Majumdar, A. and Butola, B.S. (2019), "Tailoring the mechanical and thermal properties of polylactic acid-based bio nanocomposite films using halloysite nanotubes and polyethylene glycol by solvent casting process", *J. Mater. Sci.*, **54**, 8971-8983. <https://doi.org/10.1007/s10853-019-03521-9>
- Shelly, D., Singhal, V., Jaidka, S., Banea, M.D., Lee, S.Y. and Park, S.J. (2025), "Mechanical performance of bio-based fiber reinforced polymer composites: a review", *Polym. Compos.*, **46**(S3). <https://doi.org/10.1002/pc.30000>
- Shibata, M., Ozawa, K., Teramoto, N., Yosomiya, R. and Takeishi, H. (2003), "Biocomposites made from short abaca fiber and biodegradable polyesters", *Macromol. Mater. Eng.*, **288**(1), 35-43. <https://doi.org/10.1002/mame.200290031>
- Skosana, S.J., Khoathane, C. and Malwela, T. (2025), "Driving towards sustainability: A review of natural fiber reinforced polymer composites for eco-friendly automotive light-weighting", *J. Thermoplast. Compos. Mater.*, **38**(2), 754-780. <https://doi.org/10.1177/08927057241254324>
- Srinivas, S., Ananthapadmanabha, G.S., Suresha, B., Nagarajan, R., Mohammad, F., Krishnan, K., Devi, M.I. and Ahmad, S. (2025), "Experimental studies on the physical and mechanical properties of modified silica/graphene reinforced polyamide6/copolyester elastomer blend nanocomposites", *Polym. Eng. Sci.*, **65**(2), 605-619. <https://doi.org/10.1002/pen.27028>
- Srinivasan, V.S., Boopathy, S.R., Sangeetha, D. and Ramnath, B.V. (2014), "Evaluation of mechanical and thermal properties of banana-flax based natural fibre composite", *Mater. Des.*, **60**, 620-627. <https://doi.org/10.1016/j.matdes.2014.03.014>
- Sundeep, D., Varadaraj, E.K., Ephraim, S.D., Sastry, C.C. and Krishna, A.G. (2022), "Mechanical, morphological and thermal analysis of unidirectional fabricated sisal/flax hybrid natural fiber composites", *Surf. Topograph. Metrol. Propert.*, **10**(1), 015028. <https://doi.org/10.1088/2051-672X/ac5780>
- Valapa, R.B., Pugazhenth, G. and Katiyar, V. (2015), "Effect of graphene content on the properties of poly (lactic acid) nanocomposites", *RSC Adv.*, **5**(36), 28410-28423. <https://doi.org/10.1039/C4RA15669B>
- Vasile, S., Vermeire, S., Vandepitte, K., Troch, V. and De Raeye, A. (2024), "Effect of weave and weft type on mechanical and comfort properties of hemp-linen fabrics", *Materials*, **17**(7), 1650. <https://doi.org/10.3390/ma17071650>

- Wang, L., Abenojar, J., Martínez, M.A. and Santiuste, C. (2024), "Degradation of mechanical properties of flax/PLA composites in hygrothermal aging conditions", *Polymers*, **16**(4), 528. <https://doi.org/10.3390/polym16040528>
- Wu, C.M., Lai, W.Y. and Wang, C.Y. (2016), "Effects of surface modification on the mechanical properties of Flax/ β -Polypropylene composites", *Materials*, **9**(5), 314. <https://doi.org/10.3390/ma9050314>.
- Yan, L., Chouw, N. and Yuan, X. (2012), "Improving the mechanical properties of natural fibre fabric reinforced epoxy composites by alkali treatment", *J. Reinforc. Plast. Compos.*, **31**(6), 425-437. <https://doi.org/10.1177/0731684412439494>
- Zhang, Y., Li, Y., Ma, H. and Yu, T. (2013), "Tensile and interfacial properties of unidirectional flax/glass fiber reinforced hybrid composites", *Compos. Sci. Tech.*, **88**, 172-177. <https://doi.org/10.1016/j.compscitech.2013.08.037>
- Zych, A., Perotto, G., Trojanowska, D., Tedeschi, G., Bertolacci, L., Francini, N. and Athanassiou, A. (2021), "Super tough polylactic acid plasticized with epoxidized soybean oil methyl ester for flexible food packaging", *ACS Appl. Polym. Mater.*, **3**(10), 5087-5095. <https://doi.org/10.1021/acsapm.1c00832>